Title

Finite determining parameters feedback control for distributed nonlinear dissipative systems - a computational study

Authors

Lunasin, Evelyn

Titi, Edriss S

Publication Date

2015-06-11

Peer reviewed

Finite determining parameters feedback control for distributed nonlinear dissipative systems - a computational study

Evelyn Lunasin[1] and Edriss S. Titi [2,3]

[1] Department of Mathematics, United States Naval Academy, Annapolis, MD 21402
lunasin@usna.edu

[2] Departments of Mathematics, Texas A&M University, College Station, TX 77843-3368, USA.

[3] Department of Computer Science and Applied Mathematics, The Weizmann Institute of Science, Rehovot 76100, Israel.
titi@math.tamu.edu and *edriss.titi@weizmann.ac.il*

June 11, 2015

Abstract

We present a computational study of a simple finite-dimensional feedback control algorithm for stabilizing solutions of infinite-dimensional dissipative evolution equations such as reaction-diffusion systems, the Navier-Stokes equations and the Kuramoto-Sivashinsky equation. This feedback control scheme takes advantage of the fact that such systems possess finite number of determining parameters or degrees of freedom, namely, finite number of determining Fourier modes, determining nodes, and determining interpolants and projections. In particular, the feedback control scheme uses finitely many of such observables and controllers that are acting on the coarse spatial scales. We demonstrate our numerical results for the stabilization of the unstable zero solution of the 1D Chafee-Infante equation and 1D Kuramoto-Sivashinksky equation. We give rigorous stability analysis for the feedback control algorithm and derive sufficient conditions relating the control parameters and model parameter values to attune to the control objective.

Keywords. *Chafee-Infante, Kuramoto-Sivashinksky, reaction-diffusion, Navier-Stokes equations, feedback control, data assimilation, determining modes, determining nodes, determining volume elements.*
Mathematics Subject Classification (2000): 35K57, 37L25, 37L30, 37N35, 93B52, 93C20, 93D15.

Contents

1 Introduction

Efficient algorithms for control and stabilization of flows for various transport-reaction-diffusion systems have many important applications in several areas of science and engineering. Representative applications include stabilizing flame front propagation, catalytic rod, chemical vapor deposition – a process often used in the semiconductor industry to produce thin films for defense-related applications and microelectronics manufacturing, and nonlinear control of Czochralski crystal growth processes – a well established industrial process used for the production of silicon needed in the construction of wafers for fabrication of microelectronic chips and other micro devices, to name a few (see, e.g., [9] for a detailed description of set-up and models for these industrial and engineering applications).

For several of these applications, the model equations governing its dynamics are classified as dissipative dynamical systems that are known to have a finite number of degrees of freedom. Thus, various feedback control approaches are based on reduced order models. To name some of these works, we direct the reader to [1, 2, 20, 23, 37, 52, 53, 56] and references therein. Despite many efforts, there are only a few rigorous analytical work in feedback control theory justifying these algorithms. There is also the conventional set-back on the real time implementation of these algorithms in industrial control systems.

In [4], the authors introduced a simple finite-dimensional feedback control algorithm for stabilizing solutions of infinite-dimensional dissipative evolution equations, such as reaction-diffusion systems, the Navier-Stokes equations and the Kuramoto-Sivashinsky equation. The feedback control scheme uses finitely many observables and controllers which is consistent and stems from the fact that such systems possess a finite number of determining parameters or degrees of freedom, for example, finite number of determining Fourier modes, determining nodes, and determining interpolants and projections.

We note that based on this new control algorithm a new continuous data assimilations algorithm that has applications for weather prediction was developed in [3], (see also [21, 22] for abridged continuous data assimilation). With the assumption that the observational data measurements are free of noise, the authors in [3] provided sufficient conditions on the spatial resolution of the collected coarse mesh data and the relaxation parameter that guarantees that the approximating solution obtained from this algorithm converges to the unknown reference solution over time. Then, in [6], the performance of this linear feedback control algorithm applied to data assimilations where the observational data contains stochastic measurement errors was studied. The algorithm is applied to the 2D Navier-Stokes equations. The resulting equation in the algorithm is a Navier-Stokes-like equation with stochastic feedback term that attunes the large scales in the approximate solution to those of the reference solution corresponding to the measurements. They found resolution conditions on the observational data and the relaxation/nudging parameter in which the expected value of the difference between the approximate solution, recovered by proposed linear feedback control algorithm and the exact solution is bounded by a factor which depends on the Grashof (Reynolds) number multiplied by the variance of the noise, asymptoti-

cally in time. We also note that the feedback controller proposed in [4] can be used for stabilization of the zero steady state solutions of a wide class of nonlinear dissipative wave equations, (see. eg. [42]).

In this paper, we implement the feedback control algorithm for a simple reaction-diffusion equation, the Chafee-Infante equation, which is the real version of the complex Ginzburg-Landau equation, and for the Kuramoto-Sivashinksy equation (KSE), a model for flame front propagation or flowing thin films on inclined surface. We give rigorous stability analysis for the feedback control algorithm for stabilizing the zero unstable steady state solution and derive the sufficient conditions relating the control parameters and model parameter values. The analysis for the more general case of stabilizing a nonzero reference solution of the KSE is provided in the appendix.

As an initial test case, we implement the control algorithm where the actuators are taken to be the first m Fourier modes and the control inputs prescribe the amplitude of the modes. Then, we implement the control algorithm using determining volume elements (local spatial averages) and as well as the determining volume elements based on nodal values. We also apply the algorithm for control of nonlinear parabolic PDE system to some recent feedback control case studies of the catalytic rod with or without uncertainty on the variables and give a comparison of results to existing control algorithms. For the catalytic rod with uncertainty, the control objective is the regulation of the temperature profile in the rod through the manipulation of the temperature of the cooling medium when the dimensionless heat of reaction β_T is unknown and time-varying (see pp. 102-117 in [9], for more details). In their control process there is one available control actuator and one point measurement sensor placed at the center of the rod. It was found that in the presence of uncertainty, their proposed algorithm regulates the temperature profile at the desired steady state under a certain tolerance which depends on the uncertainty level in the system parameters. We present our results on a similar computational study using the new simplified method for control of instabilities in the presence of uncertainty in the model parameters.

We note that the newly proposed feedback control for controlling general dissipative evolution equations using finitely many determining parameters like determining modes, nodes, and volume elements, is without requiring the presence of separation in spatial scales, in particular, without assuming the existence of an inertial manifold (see, eg. [53] for using inertial manifold for feedback control). In addition, it is worth mentioning that one can use this approach to show that the long-time dynamics of the underlying dissipative evolution equation, such as the two-dimensional Navier-Stokes equations, can be imbedded in an infinite-dimensional dynamical system that is induced by an ordinary differential equations, named *determining form*, which is governed by a globally Lipschitz vector field (see, e.g. [24, 25] and [38]).

2 Interpolant operators as feedback controllers

This section reviews the type of interpolant operators that we will use in our computational studies.

For $\varphi \in H^1([0,L])$ we define

$$\|\varphi\|_{H^1}^2 := \frac{1}{L^2}\int_0^L \varphi^2(x)\,dx + \int_0^L \varphi_x^2(x)\,dx. \tag{1}$$

Consider a general linear map $\mathcal{I}_h : H^1([0,L]) \to L^2([0,L])$ which is an interpolant operator that approximates the identity operator with error of order h. Specifically, it approximates the inclusion map $i : H^1 \hookrightarrow L^2$ such that the estimate

$$\|\phi - I_h(\phi)\|_{L^2} \le ch\|\phi\|_{H^1}, \tag{2}$$

holds for every $\phi \in H^1([0,L])$, where c is a dimensionless constant. The last inequality is a version of the well-known Bramble-Hilbert inequality that usually appears in the context of finite elements [10].

Examples of approximate interpolant operators, discussed in [4], with the general mapping property (see e.g., [40, 41]) mentioned above are given below.

2.1 Fourier modes

Consider a periodic function ϕ. The interpolant operator I_h acting on ϕ is defined as the projection onto the first N Fourier modes;

$$I_h(\varphi) = \frac{a_0}{2} + \sum_{k=1}^{N} a_k \cos\frac{k\pi x}{L} + \sum_{k=1}^{N} b_k \sin\frac{k\pi x}{L}, \quad h = \frac{L}{N}, \tag{3}$$

where the Fourier coefficients are given by $a_k = \frac{2}{L}\int_0^L \varphi(x)\cos\frac{k\pi x}{L}\,dx$, $\quad b_k = \frac{2}{L}\int_0^L \phi(x)\sin\frac{k\pi x}{L}\,dx$.

2.2 Finite volume elements

The volume element operator is also an interpolant operator satisfying (2). Given φ, we define

$$I_h(\varphi) = \sum_{k=1}^{N} \overline{\varphi}_k\, \chi_{_{J_k}}(x), \tag{4}$$

where $J_k = \left[(k-1)\frac{L}{N}, k\frac{L}{N}\right)$, for $k = 1,\ldots,N-1$, and $J_N = \left[(N-1)\frac{L}{N}, L\right]$, $\chi_{_{J_k}}(x)$ is the characteristic function of the interval J_k, for $k = 1,\ldots,N$, serving as the actuator shape function, and where

$$\bar{\varphi}_k = \frac{1}{|J_k|}\int_{J_k} \varphi(x)\,dx = \frac{N}{L}\int_{J_k} \varphi(x)\,dx,$$

represents the amplitude for the given actuator. Here, the local averages, $\overline{\varphi}_k$, for $k = 1, ..., N$, are the observables, which also serve as the feedback controllers.

2.3 Interpolant operator based on nodal values

We also consider here where the observables are the values $\phi(x_k^*)$, where $x_k^* \in J_k = [(k-1)\frac{L}{N}, k\frac{L}{N}]$, $k = 1, 2, \ldots, N$. In this case the feedback control scheme is given by

$$I_h(\varphi) = \sum_{k=1}^{N} \phi(x_k^*)\, \chi_{_{J_k}}(x), \quad x \in [0, L]. \tag{5}$$

where $\chi_{_{J_k}}(x)$ is the characteristic function of the interval J_k, for $k = 1, \ldots, N$, serving as the actuator shape function.

3 Motivating example: Chafee-Infante equation

We recall the Chafee-Infante reaction-diffusion equation (or the real version of the complex Ginzburg-Landau equation) on the interval $[0, L]$, with no flux boundary condition

$$\frac{\partial u}{\partial t} - \nu\, u_{xx} - \alpha u + u^3 = 0 \tag{6a}$$

$$u_x(0) = u_x(L) = 0, \tag{6b}$$

for $\alpha > 0$, large enough, and given initial condition $u(x, 0) = u_0(x)$. In [4] the authors designed a feedback control algorithm to stabilize an unstable steady state solution of (6a)-(6b) either by observing the values of the solutions at certain nodal points, local averages of the solutions in subintervals of $[0, L]$, or by observing finitely many of their Fourier modes. In the case of the steady state $\mathbf{v}(x) \equiv 0$, as a particular example, the number of feedback control needed to stabilize this zero solution is proposed (which was then rigorously justified in [4], see, also [5, 36] and [57] for a similar analysis) to be proportional to the dimension of unstable manifold which is $\sqrt{\frac{\alpha L^2}{\pi^2 \nu}}$. To shed some light on this proposed value, we linearize equation (6a) about the steady state solution $\mathbf{v} \equiv 0$, to obtain

$$\begin{aligned} &\frac{\partial \mathbf{v}}{\partial t} - \nu \mathbf{v}_{xx} - \alpha \mathbf{v} = 0, \\ &\mathbf{v}_x(0) = \mathbf{v}_x(L) = 0. \end{aligned} \tag{7}$$

One can assume a particular solution of the form $\mathbf{v}(x, t) = a_k(t)\, \cos(\frac{k\,x}{L}\pi)$, with given initial condition $\mathbf{v}_0(x) = A_k\, \cos(\frac{kx}{L}\pi)$, where $A_k \in \mathbb{R}$. Plugging in this ansatz, we obtain the equation for the time dependent coefficients as follows

$$\dot{a_k} + \nu a_k \left(\frac{\pi k}{L}\right)^2 - \alpha\, a_k = 0, \tag{8}$$

whose solution is simply

$$a_k(t) = A_k\, e^{\left(-\nu\,(\frac{\pi k}{L})^2+\alpha\right)t}.$$

One then observes that for $\alpha > 0$, large enough, all the low wave numbers $k^2 < \frac{\alpha\, L^2}{\pi^2 \nu}$ are unstable, and hence, one needs at least $\sqrt{\frac{\alpha L^2}{\pi^2 \nu}}$ number of parameters to stabilize $\mathbf{v} \equiv 0$.

3.1 Chafee-Infante equations: Finite volume elements

The following scheme was proposed as a feedback control system for (6a)-(6b) to stabilize the steady state solution $\mathbf{v} \equiv 0$:

$$\frac{\partial u}{\partial t} - \nu\, u_{xx} - \alpha u + u^3 = -\mu I_h(u) \tag{9a}$$

$$u_x(0) = u_x(L) = 0, \tag{9b}$$

where I_h is specified in section 2.

The results concerning global existence, uniqueness and stabilization for general family of finite-dimensional feedback control system that includes system (9a)-(9b) as a particular case, were established in [4]. They showed that every solution u of (9a)-(9b) tends to zero, as $t \to \infty$, under specific explicit assumptions on N, in terms of the physical parameters ν, α, L and μ. Their main results are stated in the next proposition and theorem. It is worth mentioning that similar results were first introduced and proved in [33] (see also [15] and [39]).

Proposition 3.1 ([4]). *Let $\varphi \in H^1([0, L])$ then*

$$\|\varphi(\cdot) - \sum_{k=1}^{N} \overline{\varphi}_k\, \chi_{_{J_k}}(\cdot)\|_{L^2} \;\le\; h\, \|\varphi_x\|_{L^2} \le\; h\, \|\varphi\|_{H^1}, \tag{10}$$

where $h = \frac{L}{N}$. Moreover,

$$\|\varphi\|_{L^2}^2 \le h\, \gamma^2(\varphi) + \left(\frac{h}{2\,\pi}\right)^2 \|\varphi_x\|_{L^2}^2, \tag{11}$$

where

$$\gamma^2(\varphi) = \sum_{k=1}^{N} \overline{\varphi}_k^2.$$

Using the proposition above, applying energy estimates, and giving specific explicit assumptions on N, in terms of the physical parameters ν, α, L and μ, the authors of [4] obtained the following theorem:

Theorem 3.1 ([4]). *Let N and μ be large enough such that $\mu \ge \nu \left(\frac{2\pi}{h}\right)^2 > \alpha$, where $\alpha > 0$ and $h = \frac{L}{N}$. Then $\|u(t)\|_{L^2}$ tends to zero, as $t \to \infty$, for every solution $u(t)$ of (9a)-(9b).*

Figure	# Actuators	μ	ν	α	Interpolant operator
1	0	0	1	100	
2	10	300	1	100	*finite volume elements*

Table 1: Model parameters and type of interpolant operator for the controlled and uncontrolled 1D Chafee-Infante equations

Remark 2.1

As mentioned in [4], the assumptions of Theorem 3.1, in particular, that $N > \sqrt{\frac{L^2\alpha}{4\pi^2\nu}}$, is consistent with the fact that the dimension of the unstable manifold about $\mathbf{v} \equiv 0$ is of order of $\sqrt{\frac{L^2\alpha}{\nu}}$ (see for e.g., [5, 36, 57]). It was also noted there that one can use the same idea to stabilize any other given solution, $v(x,t)$, of (6a)-(6b) by using a slightly modified feedback control in the right-hand side of (9a)-(9b) of the form $-\mu\sum_{k=1}^{N}(\overline{u}_k - \overline{v}_k)\,\chi_{_{J_k}}(x)$. Note that in [44], it was shown that the dissipative system (6a)-(6b) has only two determining close enough nodes. Whether one can design a feedback control scheme that stabilizes the zero stationary solution using only two controllers at these nodes is an open problem of an ongoing research.

3.2 Reaction-Diffusion feedback control: Numerical results

3.2.1 Discretization scheme, set-up

We solve the Chafee-Infante equation with or without feedback control, (6a)-(6b) or (9a)-(9b), respectively, with initial data $u_0 = A\cos(3x)$, with $A = 1$, supplemented with homogeneous Neumann boundary conditions using finite differences in space and explicit time stepping. We note that when $A \ll 1$, the simulation exhibits similar behavior. We solve it on the time interval $[0, 1]$, and spatial interval $[0, 1]$ and choose the step-size Δt and spatial discretization width Δx so that the ratio $r = \nu\Delta t/(\Delta x)^2 < 1/2$ for stability of the numerical scheme. We used $\alpha = 100$ and $\nu = 1$.

3.2.2 Without feedback control

The Chafee-Infante equations in the case where there is no feedback control ($\mu = 0$) has an unstable trivial steady state. Starting with some initial condition close to zero, the solution grows in time until it reaches another steady solution characterized by constant function equal to its maximum value proportional to the $\sqrt{\alpha}$ as expected.

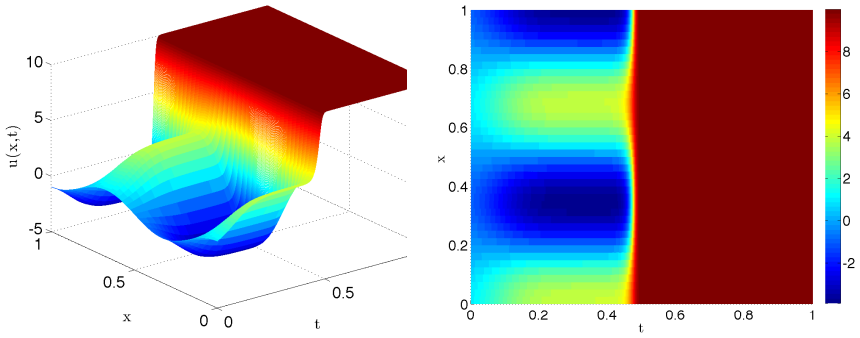

Figure 1: (a) Open-loop profile showing instability of the $u(x,t) = 0$ steady state solution. The solution increases with bound proportional to $\sqrt{\alpha}$. (b) Top-view.

3.2.3 With feedback control: Control turned on at $t = 0$.

Now we look at the numerical simulation of the control algorithm (9a)-(9b) with I_h defined as in (4) to test a simple case. We assume that measurements of the state $u(x,t)$ are available at the discretized positions and discrete times. The actuator and sensor locations are distributed uniformly throughout the domain.

To give a clear illustration, we only show the results on the time interval $[0, 0.1]$. The number of controls $NC = 10$ is consistent with the number of unstable modes $\sqrt{L^2\alpha/\nu} = 10$ with the given parameters $\alpha = 100$, $\nu = 1$, $L = 1$. The value $\mu = 300$ used in the simulation is much smaller than the value stated in Theorem 3.1. This implies that a less stringent condition is actually required than derived in the theory.

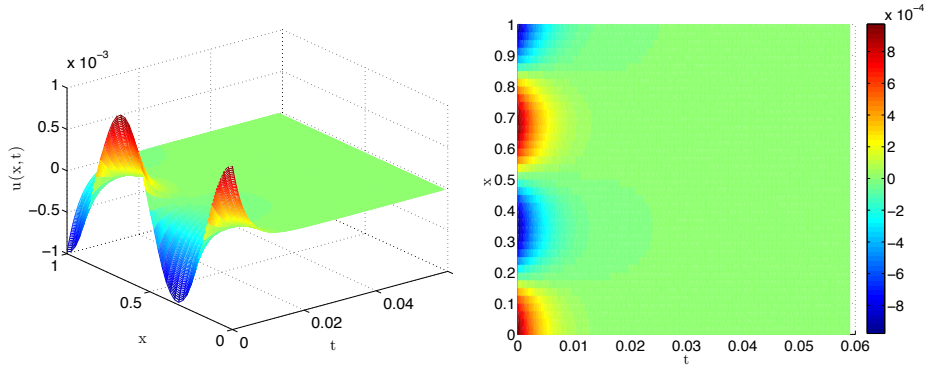

Figure 2: (a) Closed-loop profile showing stability of the $u(x,t) = 0$ steady state solution. (b) Top-view.

4 Kuramoto-Sivashinsky equation: Overview

We illustrate the application of the proposed feedback control algorithm to the stabilization of the zero solution of another nonlinear dissipative PDE known as the 1D KSE. The KSE equation was originally derived and introduced as a turbulence model for magnetized plasmas [46, 13], chemical reaction-diffusion processes [45], and flame front propagation [55]. KSE also models the motion of a thin viscous fluid or thin film flowing down an inclined wall [8]. In one space dimension, it is written as

$$\frac{\partial u}{\partial t} = -\gamma \frac{\partial^2 u}{\partial x^2} - \nu \frac{\partial^4 u}{\partial x^4} - u \frac{\partial u}{\partial x}, \quad x \in [0, L] \tag{12}$$

subject to the periodic boundary conditions, and initial condition:

$$u(x, 0) = u_0(x), \tag{13}$$

where $u(x, t)$, for example, describes the height of the film fluctuations, and the parameters γ and ν are given positive constants. Equation (12) can be nondimensionalized by substituting $u \to \gamma u/\tilde{L},\ t \to t\tilde{L}^2/\gamma,\ x \to \tilde{L}x$, and $\nu \to \tilde{L}^2\gamma\nu$, with $\tilde{L} = \dfrac{L}{2\pi}$. In this case one gets the same equation as before with the modification $\gamma = 1$ and $L = 2\pi$.

Analytical studies have revealed that the KSE also enjoys finite-dimensional asymptotic (in time) behavior (see, e.g., [11, 12, 16, 17, 26, 30, 36, 49, 51, 54, 57], and references therein). This is evident due to the fact that such systems possess finite-dimensional global attractors ([5, 16, 17, 51, 54, 57]), and finite number of determining modes ([28, 27, 26, 41]), determining nodes ([26, 31, 32, 33, 39, 41, 44]), determining volume elements ([33, 40]) and other finite number of determining parameters (degrees of freedom) such as finite elements and other interpolation polynomials ([11, 12, 32].)

Although the KSE also enjoys the property of separation of spatial scales, which guarantees the existence of a finite-dimensional inertial manifolds (see, e.g., [16, 17, 29, 30, 57], and references therein), we do not need it for the implementation of the control algorithm. Our feedback algorithm relies on the fact that the instabilities in such systems occurs solely at large spatial scales, and hence all that needed is to control these large spatial scales.

To give some justification for the choice of the number of feedback controllers (for our method the actuators and sensors are in the same locations) it is necessary to know the number of unstable modes of the steady state $\mathbf{v}(x) \equiv 0$ for a given instability parameter value ν. In order to obtain a heuristic value for the number of unstable modes, one can perform a simple analysis by linearizing equation (12) about $\mathbf{v} \equiv 0$, subject to periodic boundary conditions, to obtain the linear equation

$$\frac{\partial \mathbf{v}}{\partial t} = -\frac{\partial^2 \mathbf{v}}{\partial x^2} - \nu \frac{\partial^4 \mathbf{v}}{\partial x^4}, \quad x \in [0, 2\pi]. \tag{14}$$

Assuming a particular solution of the form $\mathbf{v}(x,t) = a_k(t)\, e^{ikx}$ yields the equation

$$\dot{a_k} = (k^2 - \nu k^4)a_k, \tag{15}$$

for the time dependent coefficients. We solve equation (15) with initial condition $\mathbf{v}_0(x) = A_k e^{ikx}$, with $A_k \in \mathbb{R}$, which yields

$$a_k(t) = A_k\, e^{k^2(1-\nu k^2)t}.$$

This shows that all the low wave numbers $k < \frac{1}{\sqrt{\nu}}$ are unstable. Thus, one needs at least $\frac{1}{\sqrt{\nu}}$ number of parameters to stabilize $\mathbf{v} \equiv 0$. Since the smaller value of ν, for which the solution $u(x,t) = 0$ is about to become unstable is $\nu = 1$, implies that the nonlinear system (12), is locally unstable when $\nu < 1$.

4.1 KSE without feedback control

4.1.1 Discretization scheme, set-up

To show some proof-of-concept corresponding to our heuristic calculations of the number of unstable modes, we present our simulations for the case where the $\nu > 1$ and the case where the $\nu < 1$. We choose the initial condition $1e^{-10} * \cos x\,(1 + \sin x)$ for both cases. Observe that for $\nu = 1.1 > 1$, our linear stability analysis shows exponential decay to the linearly stable steady state zero solution. Figure 3a is consistent with this result. The final profile of the film height is given in Figure 3b.

For the case where $\nu = 4/15 < 1$, our numerical simulation is illustrated in Figures 4a and 4b. In the context of a thin film flowing in an inclined surface, Figures 4a and 4b illustrate the unwanted wavy fluctuations that develop in time. The film height initially starts close to zero and then at around time $t = 32$ a pattern starts to evolve. At time $t = 80$, the solution is eventually attracted to a stable traveling wave. We show only up to some particular final time to display a clear transition between patterns or structures.

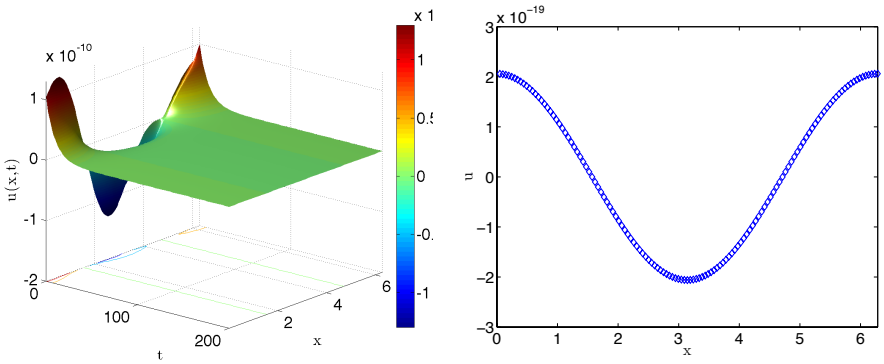

Figure 3: (a) Open-loop profile showing stability of the $u(x,t) = 0$ steady state solution when $\nu = 1.1 > 1$ (b) Profile of $u(x, t = 200)$.

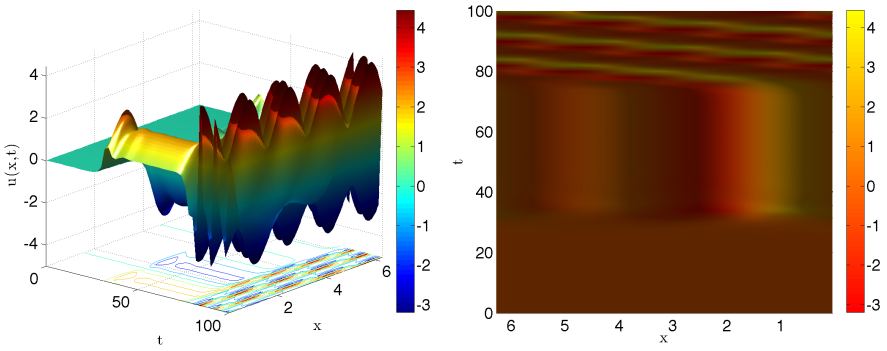

Figure 4: (a) Open-loop profile showing instability of the $u(x,t) = 0$ steady state solution when $\nu = 4/15 < 1$. (b) Top view profile of $u(x,t)$.

A common goal (see, e.g. [1], [2], [47]) is to identify a control strategy to suppress the undesirable occurrences of these wavy patterns by using actuators/sensors that control the thin film's thickness, for example, by adjusting dynamically in time a valve that serves as a source or sink at specific location in the inclined plane where the liquid film is flowing. One also needs to design a control algorithm that is likely to achieve the stabilization of the film height to the zero solution in real time making the implementation tractable for industrial control system problems.

5 KSE with feedback control

To stabilize the steady state solution $\mathbf{v} = 0$ of (12), we implement the proposed feedback control algorithm in [4], applied to KSE, which is given as follows:

$$\frac{\partial u}{\partial t} = -\frac{\partial^2 u}{\partial x^2} - \nu \frac{\partial^4 u}{\partial x^4} - u\frac{\partial u}{\partial x} - \mu\, I_h(u), \quad x \in [0, 2\pi] \tag{16}$$

subject to the periodic boundary conditions, and initial condition $u(x,0) = u_0(x)$, with $\int_0^{2\pi} u(x,0)\,dx = 0$, where the interpolant operator I_h acting on u can be defined as one of the general interpolants listed in section 2 satisfying certain properties. Note that the interpolant polynomial here is shifted by its average in the whole domain $[0, 2\pi]$ to maintain the invariance of the zero average for the controlled equation, (see e.g., equation (36) in the numerical results section below). We begin by establishing global well-posedness and stability results for the proposed feedback control algorithm.

5.1 Existence, uniqueness and stability results using finite parameters feedback control

We recall that the existence and uniqueness of solution, as well as the existence of finite-dimensional global attractor to the system (12) were first established in

[49] (see also [57]) for odd initial data. The long-time boundedness results was later improved and extended to any mean-zero initial data in [14, 35]. Improved estimates were later established in [7] and [34].

In this section we establish the global existence and uniqueness for the general feedback algorithm stated in (16); and that the I_h feedback control is stabilizing the steady state solution $\mathbf{v} \equiv 0$ of (12). This will be accomplished by choosing μ large enough and then choosing h small enough, under the assumptions

$$\mu > \frac{4}{\nu} \quad \text{and} \quad \nu > \mu\, ch^4. \tag{17}$$

Our estimates here are formal, but these steps can be justified by the Galerkin approximation procedure and then passing to the limit while using the relevant compactness theorems. We will omit the rigorous details of this standard procedure and provide only the formal *a-priori* estimates (see, e.g., [57]).

Let us now establish the aformentioned formal *a-priori* bounds for the solution which are essential for guaranteeing global existence and uniqueness.
System (16) can be rewritten as

$$\frac{\partial u}{\partial t} + \frac{\partial^2 u}{\partial x^2} + \nu \frac{\partial^4 u}{\partial x^4} + u\frac{\partial u}{\partial x} = -\mu\, I_h(u). \tag{18}$$

Taking the L^2- inner product of (18) with u, integrating by parts, and using the periodic boundary conditions, the cubic nonlinear term disappears and we obtain

$$\frac{1}{2}\frac{d}{dt}\int_0^L u^2\,dx \quad + \quad \nu \int_0^L u_{xx}^2\,dx = -\int_0^L u u_{xx}\,dx - \mu \int_0^L I_h(u)\,u\,dx.$$

Writing

$$I_h(u)\,u = (I_h(u) - u)\,u + u^2, \tag{19}$$

and applying the Cauchy-Schwarz, we get

$$\frac{1}{2}\frac{d}{dt}\int_0^L u^2\,dx + \nu \int_0^L u_{xx}^2\,dx \le \left(\int_0^L u^2\,dx\right)^{\frac{1}{2}} \left(\int_0^L u_{xx}^2\,dx\right)^{\frac{1}{2}}$$

$$- \mu \int_0^L u^2\,dx + \mu \left(\int_0^L u^2\,dx\right)^{\frac{1}{2}} \left(\int_0^L |u - I_h(u)|^2\,dx\right)^{\frac{1}{2}}.$$

Using Young's inequality, we reach

$$\begin{aligned} &\frac{1}{2}\frac{d}{dt}\|u\|_{L^2}^2 + \nu\|u_{xx}\|_{L^2}^2 \\ &\qquad \le \frac{\|u\|_{L^2}^2}{\nu} + \frac{\nu}{4}\|u_{xx}\|_{L^2}^2 - \frac{\mu}{2}\|u\|_{L^2}^2 + \frac{\mu}{2}\|u - I_h(u)\|_{L^2}^2 \end{aligned} \tag{20}$$

Let us recall the fact that for every $\phi \in H^1_{per}(0, L)$, with $\displaystyle\int_0^L \phi\,dx = 0$, (see Prop. 5 (ii) page 299 of [3]) and thanks to Poincaré inequality, one has

$$\|\phi - I_h(\phi)\|_{L^2} \le ch\,\|\phi_x\|_{L^2}, \tag{21}$$

for some constant c. Hereafter, we abuse the notation for an arbitrary constant c which may change from line to line.

Using the interpolation inequality $\|\phi_x\|_{L^2}^2 \leq \|\phi\|_{L^2}\|\phi_{xx}\|_{L^2}$ and the approximation inequality (21) one has

$$\begin{aligned}\frac{1}{2}\frac{d}{dt}\|u\|_{L^2}^2+&\frac{3\nu}{4}\|u_{xx}\|_{L^2}^2\\ &\leq \left(\frac{1}{\nu}-\frac{\mu}{2}\right)\|u\|_{L^2}+\frac{\mu}{2}ch^2\|u_x\|_{L^2}^2 \\ &\leq \left(\frac{1}{\nu}-\frac{\mu}{2}\right)\|u\|_{L^2}+\frac{\mu}{2}ch^2\|u\|_{L^2}\|u_{xx}\|_{L^2}\end{aligned} \tag{22}$$

By Young's inequality we have

$$\frac{\mu}{2}ch^2\|u\|_{L^2}\|u_{xx}\|_{L^2} \leq \frac{\mu}{4}\|u\|_{L^2}^2+\frac{\mu}{4}ch^4\|u_{xx}\|_{L^2}^2 \tag{23}$$

and substituting (23) to (22) we obtain

$$\frac{1}{2}\frac{d}{dt}\|u\|_{L^2}^2+\left(\frac{3}{4}\nu-\frac{\mu}{4}ch^4\right)\|u_{xx}\|_{L^2}^2 \leq \left(\frac{1}{\nu}-\frac{\mu}{4}\right)\|u\|_{L^2}^2 \tag{24}$$

for every $t\in[0,T)$. Thanks to the assumption (17), we have that

$$\left(\frac{3}{4}\nu-\frac{\mu}{4}ch^4\right)>0. \tag{25}$$

By dropping the $\|u_{xx}\|_{L^2}^2$ term on the left-hand side of (24) and applying Gronwall's inequality we obtain

$$\|u(t)\|_{L^2}^2 \leq e^{\left(\frac{1}{\nu}-\frac{\mu}{4}\right)t}\|u(0)\|_{L^2}^2. \tag{26}$$

In particular, by assumption (17) we find that $u\in L^\infty([0,T],L^2)$, for all $T>0$. Also notice that from (24) and (17) one can conclude that for every $\tau>0$

$$\nu\int_t^{t+\tau}\|u_{xx}(s)\|_{L^2}^2\,ds \;\leq \|u(t)\|_{L^2}^2. \tag{27}$$

Using (26) and (27) one can easily show the continuous dependence of the solutions of (16) on the initial data and the uniqueness, using similar energy estimates, provided the assumptions (21) and (17) hold.

In conclusion, from the above, and in particular thanks to (26) and (27), we have the following theorem:

Theorem 5.1. *Let μ,ν and h be positive parameters satisfying assumption (17); and that I_h satisfies (21) and $\int_0^L I_h(u)(x)\,dx=0$. Suppose $T>0$ and $u_0\in L^2([0,L])$, then system* (16) *has a unique solution $u\in C([0,T],L^2)\cap L^2([0,T],H^2)$, which also depends continuously on the initial data. Moreover,*

$$\lim_{t\to\infty}\|u(t)\|_{L^2}^2=0;$$

and for every $\tau > 0$

$$\lim_{t\to\infty} \int_t^{t+\tau} \|u_{xx}(s)\|_{L^2}^2 \, ds = 0.$$

In particular, we established (see (26)*) that under that above assumption the feedback control interpolant operator* I_h *is stabilizing the steady state solution* $v \equiv 0$ *of* (12) *in* L^2.

Remark 5.1. *In the KSE* (12)*, the term* u_{xx} *is responsible for internal destabilizing of the system, as it has been demonstrated in studying* (14)*, and the term* u_{xxxx} *is responsible for dissipating energy and stabilizes the system. In order to show that the KSE is dissipative, one takes advantage of the nonlinear term* uu_x *which transfers energy from low modes (produced by the term* u_{xx}*) to high modes which is then dissipated by the term* u_{xxxx}*. In other words, the nonlinear term is responsible for preventing the solution to growing indefinitely to infinity. On the other hand, the feedback control term is a different mechanism which stabilizes the null state. The feedback control term in* (18) *is responsible for stabilizing the low unstable modes (large spatial scales); together with* u_{xxxx} *it neutralizes the instability generated by the term* u_{xx}*. Specifically, the dissipation term* u_{xxxx} *dissipates the spillover and instabilities of the small scales that* $I_h(u)$ *might produce while stabilizing the large spatial scales.*

Remark 5.2. *Since* $\int_0^L (u_{xx}(\cdot,t))^2 \, dx < \infty$*, then* $u \in H^2$ *for a.e.* $t > 0$*. Without loss of generality, one may assume that* $u_0 \in H^2 \subset H^1$.

5.2 H^1- stability

Here we conclude that under the same assumption (17), the feedback control interpolant operator I_h is stabilizing the steady state solution $\mathbf{v} \equiv 0$ of (12) in the H^1 norm.

We start by taking the inner product of (18) with $-u_{xx}$, writing $I_h(u)$ as in (19), and integrating by parts, to get

$$\begin{aligned} \frac{1}{2}\frac{d}{dt}\int_0^L u_x^2 \, dx + \nu \int_0^L u_{xxx}^2 \, dx = &- \int_0^L u_x u_{xxx} \, dx - \frac{1}{2}\int_0^L u^2 u_{xxx} \, dx \\ &+ \mu \int_0^L (I_h(u) - u)\, u_{xx} \, dx - \mu \int_0^L u_x^2 \, dx \end{aligned} \tag{28}$$

Applying Cauchy-Schwartz and Hölder's inequality, using the fact that in one dimension, $H^1 \hookrightarrow L^\infty$, (and we have the available Agmon's inequality $\|\phi\|_{L^\infty}^2 \leq \|\phi\|_{L^2}\|\phi_x\|_{L^2}$), and then applying Young's inequality we obtain

$$\begin{aligned}
&\frac{1}{2}\frac{d}{dt}\|u_x\|_{L^2}^2 + \nu\|u_{xxx}\|_{L^2}^2 \\
&\qquad \le \|u_x\|_{L^2}\|u_{xxx}\|_{L^2} + \frac{1}{2}\|u\|_{L^\infty}\|u\|_{L^2}\|u_{xxx}\|_{L^2} \\
&\qquad\quad + \mu\|I_h(u) - u\|_{L^2}\|u_{xx}\|_{L^2} - \mu\|u_x\|_{L^2}^2 \\
&\qquad \le \frac{2\|u_x\|_{L^2}^2}{\nu} + \frac{\nu}{8}\|u_{xxx}\|_{L^2}^2 + \frac{2}{\nu}\|u\|_{L^2}^3\|u_x\|_{L^2} \\
&\qquad\quad + \frac{\nu}{8}\|u_{xxx}\|_{L^2}^2 + \mu\|u - I_h(u)\|_{L^2}\|u_{xx}\|_{L^2} - \mu\|u_x\|_{L^2}^2
\end{aligned} \tag{29}$$

Combining like terms we obtain

$$\begin{aligned}
\frac{1}{2}\frac{d}{dt}\|u_x\|_{L^2}^2 + \frac{3\nu}{4}\|u_{xxx}\|_{L^2}^2 \le \left(\frac{2}{\nu} - \mu\right)\|u_x\|_{L^2}^2 + \frac{2}{\nu}\|u\|_{L^2}^3\|u_x\|_{L^2} \\
+ \mu\|u - I_h(u)\|_{L^2}\|u_{xx}\|_{L^2}.
\end{aligned} \tag{30}$$

Notice that $\|u_{xx}\|_{L^2}^2 \le \|u_x\|_{L^2}\|u_{xxx}\|_{L^2}$ and also recall that we have (21). The right-hand side of equation (30) becomes

$$\begin{aligned}
&\le \left(\frac{2}{\nu} - \mu\right)\|u_x\|_{L^2}^2 + \frac{4}{\mu\nu^2}\|u\|_{L^2}^6 + \frac{\mu}{4}\|u_x\|_{L^2}^2 + \mu ch\|u_x\|_{L^2}^{3/2}\|u_{xxx}\|_{L^2}^{1/2} \\
&\le \left(\frac{2}{\nu} - \frac{3}{4}\mu\right)\|u_x\|_{L^2}^2 + \frac{4}{\mu\nu^2}\|u\|_{L^2}^6 + \frac{3\mu^{4/3}}{4\nu^{1/3}}ch^{4/3}\|u_x\|_{L^2}^2 + \frac{\nu}{4}\|u_{xxx}\|_{L^2}^2
\end{aligned} \tag{31}$$

(Here we used the Young's inequality $a \cdot b \le \frac{3}{4}a^{4/3} + \frac{1}{4}b^4$). Thus we have

$$\frac{1}{2}\frac{d}{dt}\|u_x\|_{L^2}^2 + \frac{\nu}{2}\|u_{xxx}\|_{L^2}^2 \le \left(\frac{2}{\nu} - \frac{3}{4}\mu + \frac{3}{4}\frac{\mu^{4/3}}{\nu^{1/3}}ch^{4/3}\right)\|u_x\|_{L^2}^2 + \frac{4}{\nu^2\mu}\|u\|_{L^2}^6 \tag{32}$$

since $\mu > \frac{4}{\nu}$ we have $\frac{2}{\nu} - \frac{3}{4}\mu \le \frac{\mu}{2} - \frac{3}{4}\mu = -\frac{\mu}{4}$. Now since $\nu > c\mu h^4$, we have $\left(\frac{\mu^4 ch^4}{\nu}\right)^{1/3} \le \frac{\mu}{4}$. It follows that the coefficient of $\|u_x\|_{L^2}$, which we denote as Q, satisfies

$$\begin{aligned}
Q := \frac{2}{\nu} - \frac{3}{4}\mu + \frac{3}{4}\frac{\mu^{4/3}}{\nu^{1/3}}ch^{4/3} &\le -\frac{\mu}{4} + \frac{3}{4}\left(\frac{\mu ch^4}{\nu}\right)^{1/3}\mu \\
&\le -\frac{\mu}{4} + \frac{3}{16}\mu < 0
\end{aligned} \tag{33}$$

We drop the positive term $\frac{\nu}{2}\|u_{xxx}\|_{L^2}^2$ in (32), recalling that $Q < 0$ and the fact that $\lim_{t\to\infty}\|u(t)\|_{L^2}^2 = 0$, we obtain from Gronwall's inequality that

$$\limsup_{t\to\infty}\|u_x(t)\|_{L^2}^2 = 0.$$

6 Numerical results: Stabilizing KSE by implementing two types of interpolant operators I_h

In this section we present the numerical results for the new feedback control algorithm (16). We illustrate through matlab computer simulations, the application of the proposed new method for stabilizing the unsteady zero solution of the Kuramoto-Sivashinksy equations. As a simple initial test case, we consider the example where the actuators are taken to be the first m modes, where m depends on the number of unstable modes and the control inputs prescribe the amplitude of the modes. We also simulate the control algorithm using determining volume elements (local spatial averages) and as well as the determining nodal values.

The stabilization of 1D KSE has been addressed in several earlier works, for example in [1], [2], and [47], in which the common starting point is reduced-order system, that can accurately describe the dynamics of the KSE. Then, from this resulting reduced-order system, the feedback controller can readily be designed and synthesized by taking advantage of the reduced-order techniques, called the approximate inertial manifold (AIM) and the proper orthogonal decomposition (POD) methods. Several other works also addressed the issue of selecting the optimal actuator/sensor placement so that the desired control energy budget are achieved with minimal cost, (see for example [48] and references therein).

We utilize a simple modification of the Exponential Time Differencing fourth-order Runge-Kutta (ETDRK4) method used to solve the KSE with feedback control. This exponential time differencing scheme was originally derived by Cox and Matthews in [18] and was later modified by Kassam and Trefethen in [43], treating the problem of numerical instability in the original scheme. This overcomes a stiff type problem via the exponential time differencing, a method which uses the idea similar to the method of integrating factor. The implementation of ETDRK4 for the KSE equation was presented as a simple example in [43]. We have adapted a similar code for a fixed computational domain, incorporated the parameter ν as the system parameter, and incorporated the feedback control term appropriately.

6.1 Case 1: Controlled KSE with finite modes

6.1.1 Projection onto Fourier modes as an interpolant operator

For a motivating simple example, we implement the proposed feedback control system in [4] for the KSE to stabilize the steady state solution $\mathbf{v} = 0$ of (12), which is given as follows:

$$\frac{\partial u}{\partial t} = -\frac{\partial^2 u}{\partial x^2} - \nu \frac{\partial^4 u}{\partial x^4} - u\frac{\partial u}{\partial x} - \mu\, I_h(u), \quad x \in [0, L] \tag{34}$$

subject to the periodic boundary conditions, with $L = 2\pi$, and initial condition $u(x, 0) = u_0(x)$, with $\int_0^L u(x, 0)\, dx = 0$, where the interpolant operator I_h acting on u is defined as in (3)

Here we do not assume any symmetry on the initial data except that its spatial average is zero. Designing the feedback control based on the first m, $L-$periodic Fourier modes, although not practical, is a common practice for testing grounds of the control method (for example, see [1, 2] and references therein). Here we present a similar initial test, that is, where feedback control is given simply by (3). We are able to implement this by modifying the definition of the operator **L** in [43] to accommodate the feedback control term $-\mu I_h$ and design a routine for the feedback control scheme that depends on the number of unstable modes and the type of interpolation operator I_h.

In Figure 5a and 5b we illustrate the solution to controlled problem using ET-DRK4. He we start with the initial condition $u_0(x) = \cos(x).*(1+\sin(x))$. The figure in 5a illustrates the open-loop profile showing instability of the $u(x,t) = 0$ steady state solution for $0 < t < 40$ for $\nu = 4/15 < 1$, then the feedback control with $\mu = 20$ is turned on for $t > 40$ which exponentially stabilizes the system. Figure 5b shows the top view profile of $u(x,t)$.

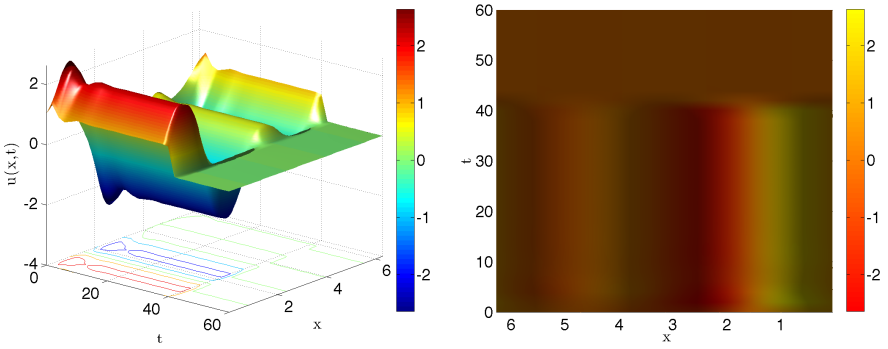

Figure 5: (a) Open-loop profile showing instability of the $u(x,t) = 0$ steady state solution for $0 < t < 40$ for $\nu = 4/15 < 1$, then the feedback control with $\mu = 20$ is turned on for $t > 40$ which exponentially stabilizes the system. (b) Top view profile of $u(x,t)$.

6.2 Case 2: Stabilizing KSE by implementing finite volume elements

Using the notation of section 3.1 we consider the proposed feedback control system in [4] to stabilize the steady state solution $\mathbf{v} = 0$ as follows:

$$\frac{\partial u}{\partial t} = -\frac{\partial^2 u}{\partial x^2} - \nu \frac{\partial^4 u}{\partial x^4} - u\frac{\partial u}{\partial x} - \mu\, I_h(u), \quad x \in [0, L], \tag{35}$$

subject to the periodic boundary conditions, with $L = 2\pi$, and initial condition $u(x,0) = u_0(x)$, where the interpolant operator acting on u, $I_h(u)$, is defined as a slight modification of (3) as follows,

$$I_h(u) = \mathcal{I}_h(u) - \langle \mathcal{I}_h(u) \rangle\,, \tag{36}$$

where $\mathcal{I}(u) = \sum_{j=1}^{N} \bar{u}_k \chi_{J_k}(x)$, and $\langle \mathcal{I}_h(u) \rangle = \dfrac{1}{L} \displaystyle\int_0^L \mathcal{I}_h u(x,t)\, dx$.

We implement this proposed control algorithm by modifying the main time-stepping loop via the 4th order Runge-Kutta in section 4 of [43] to accommodate the feedback control term $-\mu I_h$ and designing a function for the sensor/actuator placements.

6.2.1 Control turned on at $t = t_c = 0$

We denote by t_c the time when the feedback control is turned on. Figure 6 illustrates the solution to controlled problem when the control is turned on at $t = 0$. He we used the initial condition

$$u_0(x) = \left(2.5/\sqrt{5}\right) \sum_{n=1}^{5} \left(\sin(nx - n\pi) + \cos(nx - n\pi)\right). \tag{37}$$

The closed-loop profile shows exponential stabilization of the $u(x,t) = 0$ steady state solution. The number of controls is $NC = 4$, which is proportional to the number of unstable modes.

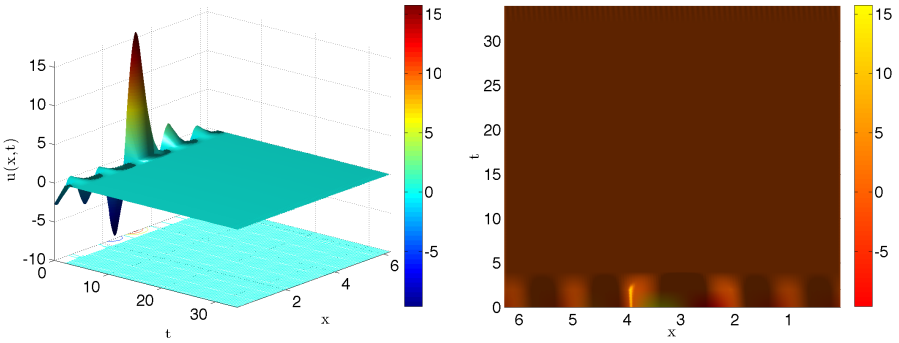

Figure 6: (a) Closed-loop profile showing fast stabilization of the $u(x,t) = 0$ steady state solution for $\nu = 4/20 < 1$, and with $\mu = 20$. (b) Top view profile of $u(x,t)$.

6.3 Case 3: Controlled KSE with interpolant operator based on nodal values

As we have mentioned earlier, designing the feedback control based on the first m, 2π-periodic Fourier modes, or based on determining volume elements may not be as practical to implement in industrial setting. This is because you would require a proportional amount of sensors or controllers as the number of grid points used in the computer simulations. Here we present a similar application of the control algorithm but where the feedback control uses (5). The amount of physical sensors or controllers one needs is proportional to the number of unstable modes for given parameter values. We are able to implement this simply by modifying

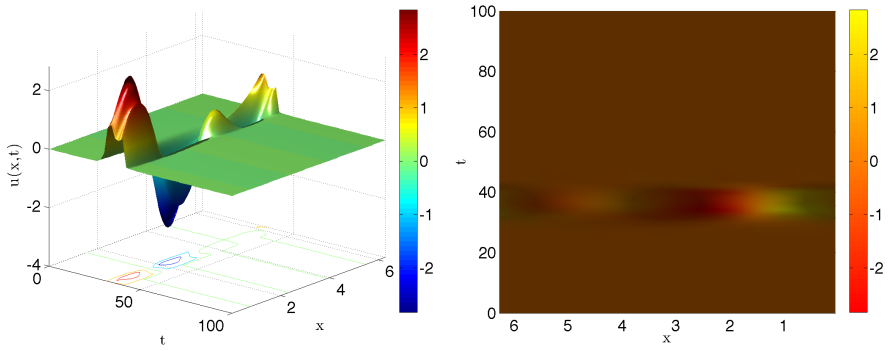

Figure 7: (a) With $u_0 = 1e^{-10}\cos x(1+\sin x)$, the film height starts to destabilize around $t = 32$ and then once feedback control is turned on at $t_c = 40$, the solution stabilizes to zero again. (b) A top view of the controlled profile.

Figure	# Actuators	μ	ν	t_c	Interpolant Operator
3	0	0	1.1	0	
4	0	0	4/15	0	
5	4	20	4/15	0	*Fourier modes*
6	4	20	4/20	0	*finite volume*
7	4	20	4/20	40	*nodal values*

Table 2: Model parameters and type of interpolant operator for the un-controlled and controlled 1D Kuramoto-Sivashinksy equations

the feedback control routine that uses the value of the function at the middle of each subintervals instead of taking the values at every discretized spatial points and then averaging them as in the previous example with the determining volume elements.

$$\frac{\partial u}{\partial t} + \frac{\partial^2 u}{\partial x^2} + \nu \frac{\partial^4 u}{\partial x^4} + u\frac{\partial u}{\partial x} = -\mu\, I_h(u), \quad x \in [0, 2\pi], \tag{38}$$

with $I_h(u)$ defined as in (5). Using similar initial condition, $u_0 = 1e^{-10}\cos x(1+\sin x)$, the same number of controllers $NC = 4$ and relaxation parameter $\mu = 20$ which is turned on at $t_c = 40$, we can see in Figure 7, that the film height starts to destabilize around $t = 32$ and then once feedback control is turned on at time $t_c = 40$ it stabilizes exponentially to zero again. We recall that the simulation time is truncated to give a clear picture of the stabilization process. We summarize our numerical experiments in Table 2.

7 Predictive control of catalytic rod with or without uncertainty variables

We illustrate the application of the proposed new method for control of nonlinear parabolic PDE system to some recent feedback control case studies of the catalytic rod. We consider the catalytic rod example introduced in [9]. Consider a long thin rod in a reactor where pure species A is fed into the system and a zeroth-order exothermic catalytic reaction of the form $A \to B$ takes place on the rod. The reaction is assumed to be exothermic which then allows the cooling medium that is in contact with the rod for decreasing the temperature. Under the assumptions of constant density and heat capacity of the rod, constant conductivity of the rod and constant temperature at both ends of the rod and unlimited supply of species A in the furnace, the model that describes the evolution of the dimensionless temperature $u(x,t)$ in the reactor as described in [9] is written as follows

$$\frac{\partial u}{\partial t} = \frac{\partial^2 u}{\partial x^2} + \beta_T e^{-\frac{\gamma}{1+u}} + \beta_U \left(b(x)q(t) - u\right) - \beta_T e^{-\gamma}, \tag{39}$$

subject to homogeneous Dirichlet boundary conditions:

$$u(0,t) = 0, \quad u(\pi,t) = 0, \tag{40}$$

and initial condition:

$$u(x,0) = u_0(x), \tag{41}$$

where β_T denotes a dimensionless heat of reaction, γ denotes a dimensionless activation energy, β_U denotes a dimensionless heat transfer coefficient, and $q(t)$ the manipulated input (supplied by the cooling medium), with $b(x)$ the actuator distribution shape function which was taken to be $b(x) = \sqrt{\frac{2}{\pi}}\sin(x)$ in [9] chosen in order to supply maximum cooling in the middle of the rod.

7.1 Case 1: Uncontrolled catalytic rod

For the typical values of the model parameters,

$$\beta_T = 50, \quad \beta_U = 2, \quad \gamma = 4, \tag{42}$$

the steady state solution $u(x,t) = 0$, when there is no control available, is unstable. Starting with an initial data with small perturbation near zero, the temperature evolves to another stable steady state where the temperature profile has a hot-spot in the middle. We run the simulation with the initial condition $u_0(x) = 1e^{-3}\sin(2x)$ on the spatial interval $[0,\pi]$ and time interval $[0,6]$. We obtain the following results illustrated in Figure 8. The axes are in units of $\Delta x = \pi/20$ and $\Delta t = 6/1000$.

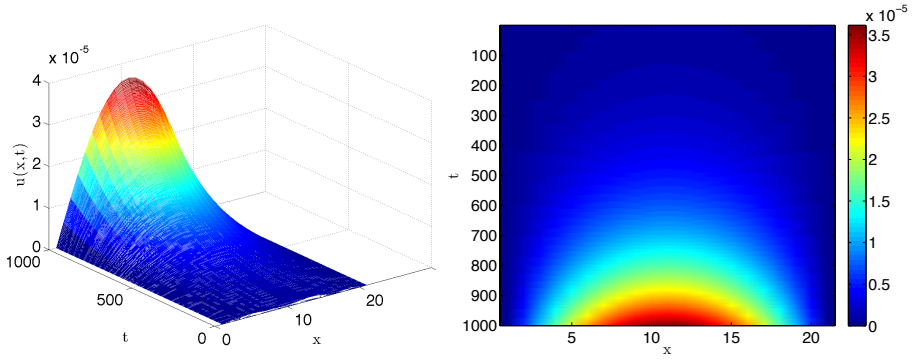

Figure 8: (a) Open-loop profile showing instability of the $u(x,t) = 0$ steady state solution. (b) Top-view of $u(x,t)$.

7.2 Case 2: Controlled catalytic rod

We now investigate the new feedback control scheme for the catalytic rod problem which takes the following form:

$$\frac{\partial u}{\partial t} = \frac{\partial^2 u}{\partial x^2} + \beta_T e^{-\frac{\gamma}{1+u}} + \beta_U \left(-\mu I_h(u) - u\right) - \beta_T e^{-\gamma}. \tag{43}$$

For the given parameters for the catalytic rod problem in (42), we observe one unstable mode and so we supply our control algorithm with $NC = 1$. We put one actuator in the middle of the rod at $x = \pi/2$. The interpolant operator is defined as $I_h(u) = \bar{u}\,\chi_{[0,\pi]}(x)$, where $\bar{u}$ is the spatial average of $u(x,t)$ on the interval $[0,\pi]$.

Under this feedback control scheme, using the same initial condition, we observed stabilization of the trivial steady state solution as shown in Figure 9.

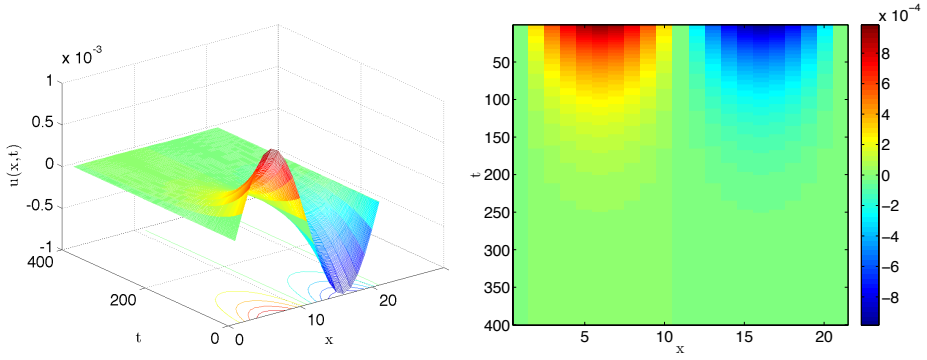

Figure 9: (a) Closed-loop profile showing stabilization to $u(x,t) = 0$ steady state solution. (b) Top-view.

7.3 Case 3: Application to catalytic rod with uncertainty

For the catalytic rod with uncertainty, the control objective is the regulation of the temperature profile in the rod through the manipulation of the temperature of the cooling medium in the presence of time-varying uncertainty in the heat of the reaction β_T (page 102 [9] for more details). The author in [9] proposed a procedure for the synthesis of the robust controllers that achieve arbitrary degree of asymptotic attenuation of the effect of the uncertain variables on the output based on the construction of higher dimensional approximation of the state slow-variables subsystems stemming from the concept of inertial manifold. Here we apply a similar study using the new feedback control algorithm.

For simplicity, we used $\beta_T = \overline{\beta}_T + \theta(t)$, where $\overline{\beta}_T = 50$ and $\theta(t) = \sin(0.524t)$. The location of the actuator is at $x = \pi/2$. In the presence of the uncertainty in some model parameters values, the control algorithm is able to compensate for the uncertainty. The result on the bounds for u depends on the size of the error in the measurements. Our results are shown in Figure 110 for the case where the initial condition has amplitude of $A = 1e^{-10}$. Although the stabilizing effect is not exponential, we see the eventual stabilization to zero.

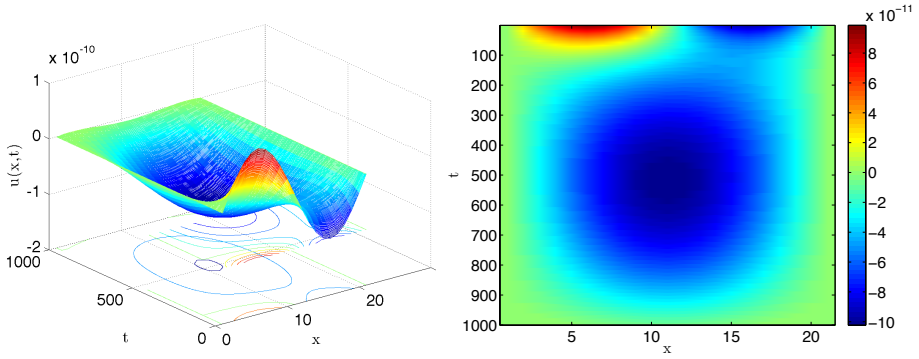

Figure 10: (a) Closed-loop profile showing eventual stability. (b) Top-view.

7.4 Case 4: Nodal-point observational measurements

For our last numerical test, we repeat Case 2 but with the feedback control scheme is given by

$$\frac{\partial u}{\partial t} = \frac{\partial^2 u}{\partial x^2} + \beta_T e^{-\frac{\gamma}{1+u}} + \beta_U \left(-\mu I_h(u) - u\right) - \beta_T e^{-\gamma}, \tag{44}$$

with $I_h(u) = u(\pi/2)\chi_{[0,\pi]}$. So the actuator and sensor are both located in the middle of the rod at $x = \pi/2$. We have observed similar behavior as in the case of the finite volume case. For this reason we do not present the figures.

We summarize our numerical experiments in Table 3.

Figure	# Actuators	μ	ν	β_T	β_U	γ	interpolant operator
8	0	0	1	50	2.0	4.0	
9	1	30	1	50	2.0	4.0	finite volume
10	1	30	1	varying	2.0	4.0	finite volume
similar to Fig 9	1	30	1	50	2.0	4.0	nodal values

Table 3: Model parameters and type of interpolant operator for the un-controlled and controlled catalytic rod problem

Acknowledgements

The work of E.L. is supported by the ONR grant N001614WX30023. The work of E.S.T. was supported in part by the ONR grant N00014-15-1-2333 and by the NSF grants DMS–1109640 and DMS–1109645. E.S.T. is also thankful to the kind hospitality of the Department of Mathematics, United States Naval Academy where this work was initiated.

8 Appendix

8.1 Existence, uniqueness and stability results for the control of solution of the KSE (general case).

In this section we will establish the global existence, uniqueness and stability results for the general feedback algorithm stated as

$$\frac{\partial u}{\partial t} + \frac{\partial^2 u}{\partial x^2} + \nu \frac{\partial^4 u}{\partial x^4} + u\frac{\partial u}{\partial x} = -\mu\,(I_h(u) - I_h(u^*)), \tag{45}$$

where I_h is a feedback control interpolant operator that is stabilizing the solution $v = u^*$ of the (12). This will be accomplished by choosing μ large enough and then choosing h small enough, under the assumptions (54), below, and that

$$\mu > \frac{4}{\nu} \quad \text{and} \quad \nu \geq \mu\, c h^4. \tag{46}$$

Under the conditions stated in (46) and (54) we derive formal *a-priori* bounds for the difference $u - u^*$ that are essential for guaranteeing the decay of $\|u - u^*\|_{L^2}$ to zero. These *a-priori* estimates, together with the global existence of u^*, form the key elements for showing the global existence of the solution u of (45). Notably, these formal steps can be justified by the Galerkin approximation procedure. Uniqueness is obtained using similar energy type estimates.

To show convergence of u to the reference solution u^*, we consider the difference $w = u - u^*$. The evolution equation for w, which is obtained by subtracting (12) and (45), is

$$w_t + \nu w_{xxxx} + w_{xx} = -ww_x - u^* w_x - wu_x^* - \mu\, I_h(w). \tag{47}$$

Multiplying by w, integrating by parts with respect to x using periodic boundary conditions (the cubic nonlinear term disappears) and using (19), we obtain

$$\begin{aligned}
&\frac{1}{2}\frac{d}{dt}\int_0^L w^2\,dx+\nu\int_0^L w_{xx}^2\,dx\\
&=-\int_0^L ww_{xx}\,dx-\int_0^L ww_x\,u^*\,dx-\frac{1}{2}\int_0^L (w^2)_x\,u^*\,dx-\mu\int_0^L I_h(w)\,w\,dx \qquad (48)\\
&=\|w_x\|_{L^2}^2+\frac{1}{2}\int_0^L w^2\,u_x^*\,dx-\mu\|w\|_{L^2}^2+\mu\int_0^L (w-I_h(w))\,w\,dx
\end{aligned}$$

A straightforward calculations, using the Poincaré, Cauchy-Schwarz, Young and Agmon ($\|\varphi\|_{L^\infty}^2\le\|\varphi\|_{L^2}\|\varphi_x\|_{L^2}$) inequalities, yield

$$\begin{aligned}
&\frac{1}{2}\frac{d}{dt}\|w\|_{L^2}^2+\nu\,\|w_{xx}\|_{L^2}^2\\
&\le\frac{2}{\nu}\|w\|_{L^2}^2+\frac{\nu}{8}\|w_{xx}\|_{L^2}^2+\frac{1}{2}\|w\|_{L^2}^2\,\|u_x^*\|_{L^\infty}-\mu\|w\|_{L^2}^2+\mu\,\|I_h(w)-w\|_{L^2}\|w\|_{L^2}\\
&\le\frac{\nu}{8}\|w_{xx}\|_{L^2}^2+\left(\frac{2}{\nu}-\mu+\|u_x^*\|_{L^\infty}\right)\|w\|_{L^2}^2+\mu ch\|w_x\|_{L^2}\|w\|_{L^2}\\
&\le\frac{\nu}{8}\|w_{xx}\|_{L^2}^2+\left(\frac{2}{\nu}-\mu+\|u_x^*\|_{L^\infty}\right)\|w\|_{L^2}^2+\mu ch\|w\|_{L^2}^{3/2}\|w_{xx}\|_{L^2}^{1/2} \qquad (49)\\
&\le\frac{\nu}{8}\|w_{xx}\|_{L^2}^2+\frac{\nu}{4}\|w_{xx}\|_{L^2}^2+\left(\frac{2}{\nu}-\mu+\|u_x^*\|_{L^\infty}\right)\|w\|_{L^2}^2+\frac{3}{4}\left(\frac{\mu^4ch^4}{\nu}\right)^{1/3}\|w\|_{L^2}^2\\
&=:Q.
\end{aligned}$$

Hereafter, we abuse the notation for an arbitrary constant c, which may change from line to line. By assumption (46) that $c\mu h^4\le\nu$ we have $\left(\frac{\mu^4ch^4}{\nu}\right)^{1/3}\le\frac{\mu}{4}$. Thus,

$$\begin{aligned}
Q&\le\frac{3\nu}{8}\|w_{xx}\|_{L^2}^2+\left(\frac{2}{\nu}-\frac{3}{4}\mu+\|u_x^*\|_{L^\infty}\right)\|w\|_{L^2}^2\\
&\le\frac{3\nu}{8}\|w_{xx}\|_{L^2}^2+\left(-\frac{\mu}{4}+\|u_x^*\|_{L^\infty}\right)\|w\|_{L^2}^2,
\end{aligned}\qquad (50)$$

where the last inequality is due to the assumption (46), i.e., $\mu>4/\nu$. In conclusion we have

$$\frac{1}{2}\frac{d}{dt}\|w\|_{L^2}^2+\frac{5}{8}\nu\,\|w_{xx}\|_{L^2}^2\le\left(-\frac{\mu}{4}+\|u_x^*\|_{L^\infty}\right)\|w\|_{L^2}^2,$$

and by Gronwall's inequality it follows that

$$\|w(t)\|_{L^2}^2\le e^{\left(-\frac{\mu}{4}+\frac{1}{t}\int_0^t\|u_x^*(s)\|_{L^\infty}\,ds\right)t}\,\|w(0)\|_{L^2}^2. \qquad (51)$$

Since u^* is a solution of KSE, it suffices to show that for large enough t we have

$$-\frac{\mu}{4}+\frac{1}{t}\int_0^t\|u_x^*(\cdot,s)\|_{L^\infty}\,ds<-\frac{\mu}{8}$$

to get an upper estimate, that decays like $e^{-\frac{\mu}{8}t}$, for $\|w(t)\|_{L^2}^2$. This can be obtained by requiring additional assumption on μ in terms of the size of the absorbing ball for KSE ([49],[57]). We then proceed noting that by Sobolev imbedding theorem in one dimension we have $\|u_x^*\|_{L^\infty} \leq \left(\frac{L}{2\pi}\right)^{1/2} \|u_{xx}^*\|_{L^2}$. From the mathematical theory of 1D KSE (see, e.g.[7, 14, 34, 49, 50, 57]) we have that

$$\limsup_{t\to\infty} \frac{1}{t} \int_0^t \|u_{xx}^*(\cdot, s)\|_{L^2}^2 \, ds = R_2^2 \tag{52}$$

where R_2 is a number which depends on the ν and L. Therefore

$$\begin{aligned} &\limsup_{t\to\infty} \frac{1}{t} \int_0^t \|u_x^*(\cdot, s)\|_{L^\infty} \, ds \\ &\qquad \leq \left(\frac{L}{2\pi}\right)^{1/2} \limsup_{t\to\infty} \left(\frac{1}{t} \int_0^t \|u_{xx}^*(\cdot, s)\|_{L^2}^2 \, ds\right)^{1/2} \leq \left(\frac{L}{2\pi}\right)^{1/2} R_2. \end{aligned} \tag{53}$$

Thus, if we assume that

$$\frac{\mu}{8} \geq \left(\frac{L}{2\pi}\right)^{1/2} R_2, \tag{54}$$

then

$$\limsup_{t\to\infty} \|w(t)\|_{L^2}^2 \leq \limsup_{t\to\infty} e^{\left(-\frac{\mu}{4} + \frac{1}{t}\int_0^t \|u_x^*(s)\|_{L^\infty} \, ds\right)t} \|w(0)\|_{L^2}^2 = 0 \tag{55}$$

We obtain the following:

Theorem 8.1. *Let μ, ν and h be positive parameters satisfying assumption* (46) *and* (54)*; and that I_h satisfies* (21) *and $\int_0^L I_h(u)(x)\, dx = 0$. Then for every $T > 0$ and $u_0 \in L^2([0, L])$, system* (45) *has a unique solution $u \in C([0, T], L^2) \cap L^2([0, T], H^2)$, which also depends continuously on the initial data. Moreover,*

$$\lim_{t\to\infty} \|u(t) - u^*\|_{L^2}^2 = 0;$$

and for every $\tau > 0$

$$\lim_{t\to\infty} \int_t^{t+\tau} \|u_{xx}(s) - u_{xx}^*\|_{L^2}^2 \, ds = 0.$$

The stability in H^1 can be obtained by a slight modification of the previous analysis. Here we conclude that under the assumption (46) and (54), the feedback control interpolant operator I_h is stabilizing the steady state solution $v \equiv u^*$ of (12) in the H^1 norm. Taking the inner product of (47) with $-w_{xx}$, writing $I_h(u)$ as in (19) and integrating by parts, yields

$$\begin{aligned} &\frac{1}{2}\frac{d}{dt} \int_0^L w_x^2 \, dx + \nu \int_0^L w_{xxx}^2 \, dx \\ &\quad = -\int_0^L w_x w_{xxx} \, dx - \frac{1}{2} \int_0^L u_x^* (w_x)^2 \, dx - \frac{1}{2} \int_0^L w^2 w_{xxx} \, dx \\ &\quad + \int_0^L u_x^* (w w_{xx}) \, dx + \mu \int_0^L (I_h(w) - w)\, w_{xx} \, dx - \mu \int_0^L w_x^2 \, dx \end{aligned} \tag{56}$$

Applying Cauchy-Schwarz, Hölder's, Agmon and Gagliardo-Nirenberg interpolation ($\|\phi_{xx}\|_{L^2}^2 \leq \|\phi_x\|_{L^2}\|\phi_{xxx}\|_{L^2}$) inequalities, and then applying Young inequality, we obtain

$$\begin{aligned}
&\frac{1}{2}\frac{d}{dt}\|w_x\|_{L^2}^2 + \nu\|w_{xxx}\|_{L^2}^2 \\
&\quad\leq \|w_x\|_{L^2}\|w_{xxx}\|_{L^2} + \frac{1}{2}\|u_x^*\|_{L^\infty}\|w_x\|_{L^2}^2 + \frac{1}{2}\|w\|_{L^\infty}\|w\|_{L^2}\|w_{xxx}\|_{L^2}, \\
&\qquad + \|u_x^*\|_{L^\infty}\|w\|_{L^2}\|w_{xx}\|_{L^2} + \mu\|I_h(w) - w\|_{L^2}\|w_{xx}\|_{L^2} - \mu\|w_x\|_{L^2}^2 \\
&\quad=: Q_1 + Q_2 + Q_3 + Q_4 + Q_5 + Q_6,
\end{aligned} \tag{57}$$

with

$$\begin{aligned}
Q_1 &= \|w_x\|_{L^2}\|w_{xxx}\|_{L^2} \leq \frac{1}{\nu}\|w_x\|_{L^2}^2 + \frac{\nu}{4}\|w_{xxx}\|_{L^2}^2, \\
Q_2 &= \frac{1}{2}\|u_x^*\|_{L^\infty}\|w_x\|_{L^2}^2, \\
Q_3 &= \frac{1}{2}\|w\|_{L^\infty}\|w\|_{L^2}\|w_{xxx}\|_{L^2} \leq \frac{1}{2}\|w\|_{L^2}^{3/2}\|w_x\|_{L^2}^{1/2}\|w_{xxx}\|_{L^2} \\
&\leq \frac{1}{4\nu}\|w\|_{L^2}^3\|w_x\|_{L^2} + \frac{\nu}{4}\|w_{xxx}\|_{L^2}^2 \\
&\leq \frac{1}{2\mu\nu^2}\|w\|_{L^2}^6 + \frac{\mu}{16}\|w_x\|_{L^2}^2 + \frac{\nu}{4}\|w_{xxx}\|_{L^2}^2, \\
Q_4 &= \|u_x^*\|_{L^\infty}\|w\|_{L^2}\|w_{xx}\|_{L^2} \leq \|u_x^*\|_{L^\infty}^2\frac{h^2}{4\nu}\|w\|_{L^2}^2 + \frac{\nu}{h^2}\|w_{xx}\|_{L^2}^2 \\
Q_5 &= \mu\|I_h(w) - w\|_{L^2}\|w_{xx}\|_{L^2} \leq \mu ch\|w_x\|_{L^2}\|w_{xx}\|_{L^2} \\
&\leq \frac{\mu}{16}\|w_x\|_{L^2}^2 + \mu ch^2\|w_{xx}\|_{L^2}^2 \leq \frac{\mu}{16}\|w_x\|_{L^2}^2 + \frac{\nu}{h^2}\|w_{xx}\|_{L^2}^2, \\
Q_6 &= -\mu\|w_x\|_{L^2}^2,
\end{aligned} \tag{58}$$

where for Q_5, we used the approximation identity (21) and the assumption (46) that $\nu \geq \mu\, ch^4$. Collecting like terms we have

$$\begin{aligned}
\frac{1}{2}\frac{d}{dt}\|w_x\|_{L^2}^2 + \frac{\nu}{2}\|w_{xxx}\|_{L^2}^2 \leq &\left(\frac{1}{\nu} - \mu + \frac{\mu}{8} + \|u_x^*\|_{L^\infty}\right)\|w_x\|_{L^2}^2 \\
&+ \frac{1}{2\mu\nu^2}\|w\|_{L^2}^6 + \frac{h^2}{4\nu}\|u_x^*\|_{L^\infty}^2\|w\|_{L^2}^2 + \frac{2\nu}{h^2}\|w_{xx}\|_{L^2}^2.
\end{aligned} \tag{59}$$

By assumption (46), that $\mu > \dfrac{4}{\nu}$, we have

$$\begin{aligned}
\frac{d}{dt}\|w_x\|_{L^2}^2 + \nu\|w_{xxx}\|_{L^2}^2 \leq &\, 2\left(-\frac{\mu}{2} + \|u_x^*\|_{L^\infty}\right)\|w_x\|_{L^2}^2 \\
&+ \frac{1}{\mu\nu^2}\|w\|_{L^2}^6 + \frac{h^2}{2\nu}\|u_x^*\|_{L^\infty}^2\|w\|_{L^2}^2 + \frac{4\nu}{h^2}\|w_{xx}\|_{L^2}^2.
\end{aligned} \tag{60}$$

Let $\epsilon > 0$ be a given arbitrarily small number. Thanks to Theorem 8.1 there exists a $T_0(\epsilon) > 0$, large enough, such that for all $t \geq T_0$ we have

$$\|w(t)\|_{L^2} < \epsilon, \quad \int_t^{t+\tau}\|w_{xx}(s)\|_{L^2}^2 ds < K\epsilon, \quad \text{and} \quad \|u_x^*\|_{L^\infty} \leq 2\left(\frac{L}{2\pi}\right)^{1/2} R_2. \tag{61}$$

Thus, for $t \geq T_0 + \tau$ we have

$$\begin{aligned}\frac{d}{dt}\|w_x\|_{L^2}^2 + \nu\|w_{xxx}\|_{L^2}^2 \leq 2\left(-\frac{\mu}{2} + \|u_x^*\|_{L^\infty}\right)\|w_x\|_{L^2}^2 + \\ + \frac{1}{\mu\nu^2}\epsilon^6 + \frac{2h^2}{\nu}R_2^2\,\epsilon^2 + \frac{4\nu}{h^2}\|w_{xx}\|_{L^2}^2.\end{aligned} \tag{62}$$

By assumption (54) and Gronwall inequality we have

$$\begin{aligned}\|w_x(t)\|_{L^2}^2 \leq e^{-\frac{\mu}{2}(t-T_0)}\|w_x(T_0)\|_{L^2}^2 + \frac{2}{\mu}\left(\frac{1}{\mu\nu^2}\epsilon^6 + \frac{2h^2}{\nu}R_2^2\,\epsilon^2\right)\left(e^{-\frac{\mu}{2}T_0} - e^{-\frac{\mu}{2}t}\right) \\ + \frac{4\nu}{h^2}\int_{T_0}^t e^{-\frac{\mu}{2}(t-s)}\|w_{xx}(s)\|_{L^2}^2\,ds.\end{aligned} \tag{63}$$

Let us treat the integral $J = \displaystyle\int_{T_0}^t e^{-\frac{\mu}{2}(t-s)}\|w_{xx}(s)\|_{L^2}^2\,ds$. There exists a natural number N such that $T_0 + N\tau \leq t < T_0 + (N+1)\tau$. Therefore,

$$\begin{aligned}J &\leq \int_{T_0}^{T_0+(N+1)\tau} e^{-\frac{\mu}{2}(t-s)}\|w_{xx}(s)\|_{L^2}^2\,ds \\ &= \sum_{k=0}^{N}\int_{T_0+k\tau}^{T_0+(k+1)\tau} e^{-\frac{\mu}{2}(t-s)}\|w_{xx}(s)\|_{L^2}^2\,ds \\ &\leq \sum_{k=0}^{N} e^{-\frac{\mu}{2}(t-(k+1)\tau-T_0)}\int_{T_0+k\tau}^{T_0+(k+1)\tau}\|w_{xx}(s)\|_{L^2}^2\,ds \\ &\leq K\epsilon\, e^{-\frac{\mu}{2}(t-T_0)}\sum_{k=0}^{N} e^{\frac{\mu}{2}(k+1)\tau} \\ &\leq K\epsilon\, e^{-\frac{\mu}{2}(t-T_0)}\left(\frac{e^{\frac{\mu}{2}(N+1)\tau}-1}{e^{\frac{\mu}{2}\tau}-1}\right)e^{\frac{\mu}{2}\tau}\end{aligned} \tag{64}$$

Notice that

$$e^{-\frac{\mu}{2}(t-T_0)}e^{\frac{\mu}{2}(N+1)\tau} = e^{\frac{\mu}{2}(T_0+(N+1)\tau-t)} \leq e^{\frac{\mu}{2}\tau}$$

and

$$e^{-\frac{\mu}{2}(t-T_0)} \geq 0.$$

Thus, $J \leq K\epsilon\left(\frac{e^{\mu\tau}}{e^{\frac{\mu}{2}\tau}-1}\right)$. Using the upper bound for J and noting that $e^{-\frac{\mu}{2}T_0} - e^{-\frac{\mu}{2}t} \leq 1$, we obtain from (63), that for $t \geq T_0 + \tau$,

$$\|w_x(t)\|_{L^2}^2 \leq e^{-\frac{\mu}{2}(t-T_0)}\|w_x(T_0)\|_{L^2}^2 + \tfrac{2}{\mu}\left(\tfrac{1}{\mu\nu^2}\epsilon^6 + \tfrac{2h^2}{\nu}R_2^2\,\epsilon^2\right) + \tfrac{4\nu}{h^2}K\epsilon\left(\tfrac{e^{\mu\tau}}{e^{\frac{\mu}{2}\tau}-1}\right).$$

Taking the limit supremum as $t \to \infty$ we get

$$\limsup_{t\to\infty} \|w_x(t)\|_{L^2}^2 \leq \frac{2}{\mu}\left(\frac{1}{\mu\nu^2}\epsilon^6 + \frac{2h^2}{\nu}R_2^2\,\epsilon^2\right) + \frac{4\nu}{h^2}K\epsilon\left(\frac{e^{\mu\tau}}{e^{\frac{\mu}{2}\tau}-1}\right).$$

We let $\epsilon \to 0$ to obtain

$$\limsup_{t\to 0} \|w_x(t)\|_{L^2}^2 = 0, \quad \text{hence,} \quad \lim_{t\to 0} \|w_x(t)\|_{L^2}^2 = 0.$$

References

[1] S. Ahuja, *Reduction Methods for Feedback Stabilization of Fluid Flows*, Ph.D Thesis, Dept. of Mechanical and Aerospace Engineering, Princeton University, 2009.

[2] A. Armaou and P. D. Christofides, *Feedback control of the Kuramoto-Sivashinsky equation*, Physica D **137**, Issues 1-2, pp. 49–61 (2000).

[3] A. Azouani, E. Olson and E.S. Titi, *Continuous data assimilation using general interpolant observables*, J. Nonlinear Sci., **24**, pp. 277–304 (2014).

[4] A. Azouani, and E.S. Titi, *Feedback control of nonlinear dissipative systems by finite determining parameters - A reaction-diffusion Paradigm*, Evolution Equations and Control Theory, **3**:579 (2014).

[5] A. V. Babin and M. Vishik, *Attractors of Evolutionary Partial Differential Equations*, North-Holland, Amsterdam, London, NewYork, Tokyo, (1992).

[6] H. Bessaih, E. Olson and E.S. Titi, *Continuous assimilation of data with stochastic noise*, Nonlinearity, **28**, pp. 729-753 (2015).

[7] J. Bronski and T. Gambill, *Uncertainty estimates and L_2 bounds for the Kuramoto-Sivashinsky equation*, Nonlinearity, **19**, pp. 2023–2039 (2006).

[8] L.H. Chen, and H.C. Chang *Nonlinear waves on liquid film surfaces-II. Bifurcation analyzes of the long-wave equation*, Chem. Eng. Sci., **41**, pp. 2477–2486 (1986).

[9] P. D. Christofides, *Nonlinear and robust control of PDE systems: Methods and Applications to Transport-Reaction Processes*, Springer Science + Business Media, New York (2001).

[10] P. G. Ciarlet, *The Finite Element Method for Elliptic Problems*, Classics in Applied Mathematics, **40**, SIAM, (2002).

[11] B. Cockburn, D.A. Jones, E.S. Titi, *Degrés de liberté déterminants pour équations non linéaires dissipatives*, C.R. Acad. Sci.-Paris, Sér. I **321**, pp. 563–568 (1995).

[12] B. Cockburn, D.A. Jones and E.S., Titi, *Estimating the number of asymptotic degrees of freedom for nonlinear dissipative systems*, Math. Comput. **97**, pp. 1073–1087 (1997).

[13] B.I. Cohen, J.A. Krommes, W.M. Tang and M.N. Rosenbluth, *Non-linear saturation of the dissipative trapped-ion mode by mode coupling*, Nuclear Fusion **16:6**, pp. 971–974 (1976).

[14] P. Collet, J-P. Eckmann, H. Epstein and J. Stubbe., *A global attracting set for the Kuramoto-Sivashinksy equation*, Commun. Math. Phys., **152**, pp. 203–214 (1993).

[15] P. Constantin, Ch. Doering and E.S. Titi, *Rigorous estimates of small scales in turbulent flows*, Journal of Mathematical Physics **37**, pp. 6152-6156 (1996).

[16] P. Constantin and C. Foias, *Navier-Stokes Equations*, University of Chicago Press, Chicago, (1988).

[17] P. Constantin, C. Foias, B. Nicolaenko and R. Temam, *Integral Manifolds and Inertial Manifolds for Dissipative Partial Differential Equations*, Springer-Verlag, Applies Mathematical Sciences Series, Vol. **70** (1988).

[18] S.M. Cox and P.C. Matthews, *Exponential time differencing for stiff systems*, J. Comput. Phys. **176**, pp. 430-455, (2002).

[19] S. Dubljevic, P Mhaskas, N. El-Farra, P. Christofides, *Predictive control of transport-reaction processes*, Computers and Chemical Engineering **29**, pp. 2335–2345 (2005)

[20] N. H. El-Farra, A. Armaou and P.D. Christofides, *Analysis and control of parabolic PDE systems with input constraints*, Automatica **39:4**, pp. 715–725 (2003).

[21] A. Farhat, M. S. Jolly and E. S. Titi, *Continuous data assimilation for the 2D Bénard convection through velocity measurements Alone*, Physica D, **303**, pp. 59–66 (2015).

[22] A. Farhat, E. Lunasin, and E.S. Titi *Abridged continuous data assimilation for the 2D Navier-Stokes Equations utilizing measurements of only one component of the velocity field*, submitted, arXiv:1504.05978v1, (2015).

[23] C. Foias, M.S. Jolly, I.G. Kevrekidis, G.R. Sell and E.S. Titi, *On the computation of inertial manifolds*, Physics Letters A **131**, pp. 433–436 (1988).

[24] C. Foias, M. Jolly, R. Kravchenko and E.S. Titi, *A determining form for the 2D Navier-Stokes equations - the Fourier modes case*, Journal of Mathematical Physics **53**, pp. 115623-1–115623-30 (2012).

[25] C. Foias, M. Jolly, R. Karavchenko and E.S. Titi, *A unified approach to determining forms for the 2D Navier-Stokes equations – the general interpolants case*, Russian Mathematical Surveys **69:2**, pp. 359–381 (2014).

[26] C. Foias, O.P. Manley, R. Rosa, R. Temam, *Navier-Stokes Equations and Turbulence*, Cambridge University Press, 2001.

[27] C. Foias, O.P. Manley, R. Temam and Y. Treve, *Asymptotic analysis of the Navier-Stokes equations*, Physica D **9**, pp. 157–188 (1983).

[28] C. Foias, G. Prodi, *Sur le comportement global des solutions non stationnaires des équations de Navier-Stokes en dimension deux*, Rend. Sem. Mat. Univ. Padova **39**, pp. 1–34 (1967).

[29] C. Foias, G.R. Sell and R. Temam, *Inertial manifolds for nonlinear evolutionary equations*, Journal of Differential Equations **73**, pp. 309–353 (1988).

[30] C. Foias, G.R. Sell and E.S. Titi, *Exponential tracking and approximation of inertial manifolds for dissipative nonlinear equations*, Journal of Dynamics and Differential Equations **1**, pp. 199–244 (1989).

[31] C. Foias and R. Temam, *Determination of the solutions of the Navier-Stokes equations by a set of nodal values*, Math. Comput. **43**, pp. 117–133 (1984).

[32] C. Foias, R. Temam, *Asymptotic numerical analysis for the Navier-Stokes equations*, Nonlinear Dynamics and Turbulence, Edit. by Barenblatt, Iooss, Joseph, Boston: Pitman Advanced Pub. Prog., (1983).

[33] C. Foias and E.S. Titi, *Determining nodes, finite difference schemes and inertial manifolds*, Nonlinearity **4**, pp. 135–153 (1991).

[34] L. Giacomeli and F. Otto, *New bounds for the Kuramoto-Sivashinsky equation*, Commun. Pure. Appl. Math., **58**, pp. 297–318 (2005).

[35] J. Goodman, *Stability of the Kuramoto-Sivashinky and related systems*, Commun. Pure Appl. Math. **47**, pp. 293–306 (1994).

[36] J. K. Hale, *Asymptotic behavior of dissipative Systems, Math. Survey and Monographs*, **25**, AMS, Providence, R. I. (1988).

[37] M.S. Jolly, and I.G. Kevrekidis and E.S. Titi, *Approximate inertial manifolds for the Kuramoto–Sivashinsky equation: Analysis and Computations*, Physica D **44**, pp. 38–60 (1990).

[38] M.S. Jolly, T. Sadigov and E.S. Titi, *A determining form for the damped driven nonlinear Schrödinger equation- Fourier modes case*, J. Diff. Eqns., **258:8**, pp. 2711-2744 (2015).

[39] D. Jones and E.S. Titi, *On the number of determining nodes for the 2-D Navier-Stokes equations*, J. Math. Anal. Appl. vol. **168:1**, pp. 72–88 (1992).

[40] D. Jones and E.S. Titi, *Determining finite volume elements for the 2-D Navier–Stokes equations*, Physica D **60**, pp. 165–174 (1992).

[41] D. Jones and E.S. Titi, *Upper bounds on the number of determining modes, nodes, and volume elements for the Navier-Stokes equations*, Indiana University Mathematics Journal **42**, pp. 875-887 (1993).

[42] V. Kalantarov and E.S. Titi, *Finite-parameters feedback control for stabilizing damped nonlinear wave equations*, Contemporary Mathematics, volume on "Nonlinear Analysis and Optimization", AMS, (2015), (to appear). arXiv:1501.00556.

[43] A. Kazaam and L. Trefethen, *Fourth-order time stepping for stiff PDEs*, J. Sci Comp. **26**, pp. 1214–1233 (2005).

[44] I. Kukavica, *On the number of determining nodes for the Ginzburg-Landau equation*, Nonlinearity **5**, pp. 997–1006 (1992).

[45] Y. Kuramoto and T. Tsusuki, *Reductive perturbation approach to chemical instabilities*, Prog. Theor. Phys. **52**, pp. 1399–1401 (1974).

[46] R. E. LaQuey, S. M. Mahajan, P. H. Rutherford, and W. M. Tang, *Nonlinear saturation of the trapped-ion mode*, Phys. Rev. Let. **34**, pp. 391–394 (1975).

[47] C.H. Lee, H.T. Tran, *Reduced-order-based feedback control of the Kuramoto-Sivashinsky equation*, Journal of Computational and Applied Mathematics **173:1**, pp. 1–19 (2005).

[48] Y. Lou, P. Christofides, *Optimal actuator/sensor placement for nonlinear control of the Kuramoto-Sivashinksky equation*, IEEE Transactions on Control Systems Tech. **11:5**, pp. 737–745 (2002).

[49] B. Nicolaenko, B. Scheurer, and R. Temam, *Some global dynamical properties of the Kuramoto-Sivashinsky equation: nonlinear stability and attractors*, Physica D **16**, pp. 155-183 (1985).

[50] F. Otto, *Optimal bounds on the Kuramoto-Sivashinsky equations*, Journal of Functional Analysis, **257:7**, pp. 2188-2245 (2009).

[51] J. Robinson, *Infinite-Dimensional Dynamical Systems: An Introduction to Dissipative Parabolic PDEs and the Theory of Global Attractors*, Cambridge Texts in Applied Mathematics, (2001).

[52] R. Rosa *Exact finite-dimensional feedback control via inertial manifold theory with application to the Chafee-Infante equation*, J. Dynamics and Diff. Eqs. **15:1**, pp. 61–86 (2003).

[53] R. Rosa and R. Temam, *Finite-dimensional feedback control of a scalar reaction-diffusion equation via inertial manifold theory*, in Foundations of Computational Mathematics, Selected papers of a conference held at IMPA, Rio de Janeiro, RJ, Brazil, January 1997 (Eds. F. Cucker and M. Shub), pp. 382–391, Springer-Verlag, Berlin (1997).

[54] G.R. Sell, Y. You, *Dynamics of Evolutionary Equations*, Springer, 2002.

[55] G.I. Sivashinsky, *Nonlinear analysis of hydrodynamic instability in laminar flames*, Acta Astronautica **4**, pp. 1177-1206 (1977).

[56] S. Shvartsman, C. Theodoropoulos, R. Rico-Martinez, I.G. Kevrekidis, E.S. Titi, and T.J. Mountziares, *Order reduction of nonlinear dynamic models for distributed reacting systems*, Journal of Process Control **10**, pp.177–184 (2000).

[57] R. Temam, *Infinite Dimensional Dynamical Systems in Mechanics and Physics*, New York: Springer (1988).

[58] R. Temam, *Navier-Stokes Equations: Theory and Numerical analysis*, AMS Chelsea Publishing, Providence, RI, Theory and numerical analysis, Reprint of the 1984 edition. (2001).